

# BEHAVIOR OF FLAT SLAB–COMPOSITE COLUMN CONNECTIONS

Ahmed A. Mahmoud<sup>1</sup>, Gamal T. Abdel Rahman<sup>2</sup>, Haitham M. Fawzi<sup>3</sup>

<sup>1</sup>Professor and Head of Civil Eng. Dept, <sup>2</sup>Assistance Professor, <sup>3</sup>Civil Eng. and Master Student  
Civil Engineering Department, Faculty of Engineering at Shoubra, Benha University.

## ABSTRACT

This paper presented a proposal for a new reinforcing system to improve punching shear resistance of composite column-flat slab connections. Results on thirteen specimens tested under vertical static loading are presented. The influence of the slab thickness and the steel system characteristics were considered. In addition, a non-linear finite elements analysis was carried out using ANSYS code. The key parameters namely the concrete compressive strength, steel reinforcement yield strength, column rectangularity ratio, slab rectangularity ratio, tension steel reinforcement ratio, and steel system characteristics were investigated through a parametric study adopting NLFEA.

Test results revealed enhancement in the failure load ranging between 2.53% and 33.5% for the specimens provided with the suggested reinforcing system. In general, the punching shear resistance increased by increasing the reinforcing angles length, while changing the steel section shape inside the composite column had no significant effect on the failure load.

**KEYWORDS:** Reinforced Concrete; Experimental Investigations, Nonlinear Behavior; Punching Shear; Analytical Study; Numerical Analysis; Composite Columns; Flat Slabs; Connections.

## ملخص البحث :

يعرض هذا البحث اقتراح نظام جديد من القطاعات الحديدية لتحسين مقاومة القص الثاقب للأعمدة المركبة من قطاعات حديدية مغلقة بالخرسانة عند اتصالها بأسقف من البلاطات الخرسانية المسلحة المسطحة (اللاكمرية). ثلاثة عشر عينة تم اختبارهم تحت تأثير تحميل رأسي مركزي بالإضافة لعمل دراسة نظرية باستخدام برنامج التحليل الإنشائي الغير خطي "ANSYS". وقد تم استخدام برنامج التحليل الإنشائي الغير خطي "ANSYS" في عمل دراسة بارامترية لدراسة العديد من العوامل مثل مقاومة الخرسانة في الضغط، إجهاد خضوع حديد التسليح، نسبة طول العمود إلى عرضه، نسبة طول البلاطة الخرسانية إلى عرضها، نسبة التسليح السفلي للبلاطة، وخصائص النظام الحديدي المقترح.

أظهرت النتائج المعملية تعزيز في حمل الانهيار يتراوح بين 2.35% إلى 33.5% للعينات المدعومة بالنظام الحديدي المقترح. بشكل عام تتحسن مقاومة القص الثاقب بزيادة أطوال زوايا النظام الحديدي بينما لا يوجد تأثير على حمل الانهيار عند تغيير شكل القطاع الحديدي داخل العمود المركب.

## **1- INTRODUCTION**

For high rise buildings, especial columns with concrete filled hollow sections and additional massive inner steel core sections are used in order to get a very high resistance to normal forces and simultaneously with regard to architectural design small dimensions of the columns. Furthermore, the combination of these types of composite columns with flat concrete slabs without localized thickening of slab leads to very economic solutions, because very simple formwork can be used for the slabs and optimal conditions exist for the mechanical services of the building. Under these boundary conditions, the punching shear resistance of the flat slab may become critical.

In order to increase the resistance to punching shear in concrete structures, often special shear reinforcement systems or head studs are used. In case of very high punching shear loads, shear heads consisting of steel profiles integrated in the slab are used. The main aim is to increase resistance to punching shear and improve the deformation capacity and ductility in order to get a significant redistribution of bending moments and internal forces in flat slab systems. In these systems, the composite action is obtained by a combination of headed studs and special steel-endplates at the end of the shear legs. Within the last few years, this system was already used for slabs in multistory buildings and also for increasing the punching shear resistance in flat basement slabs.

In this paper, a new steel system was suggested to be used at the middle of the concrete flat slab thickness. The new steel system was applied by using four steel angles welded tightly with the steel column section. The number of steel rows was taken as a variable parameter at the experimental tests.

## **2- RESEARCH SIGNIFICANCE**

Thorough literature review revealed little applicable research on the topic of composite columns-flat slab connection. A study by Piel W. and Hanswille G. (2006) testing the effect of shear head systems on improving punching shear resistance of flat slab-composite column connection which was the only found related with this topic. Otherwise none composite column-flat slab connection have been widely researched and documented.

There have been extensive experimental investigations of non-composite column-flat slab connections (Swamy R. N. and Ali S. A. R. (1982), Bazant Z. P. and Cao Z. (1987), Osman M., Marzouk H., and Helmy S. (2000), Oliveira D. R., Melo G. S., and Regan P. E. (2000), Vainiūnas P., Popovas V. and Jarmolajev A. (2002), Ospina C. E., Alexander S. D. B., and Cheng J. J. R. (2003), El-Salakawy E. F., Polak M. A., and Soudki K. A. (2003), Hegger J., Sherif A. G., and Ricker M. (2006), Duarte I., Ramos A. M. P., and Lúcio V. J. G. (2008), Mirzaei Y. (2008), Kheyroddin A., Vaez S. R. H., and Naderpour H. (2008)).

Therefore, this paper provides an attempt to study experimentally and numerically the behavior of composite column-flat slab connection under vertical loading after strengthened by a new suggested steel system.

### **3- EXPERIMENTAL PROGRAM**

#### **3.1 Test specimens**

The specimens were constructed to model flat slab – composite column connection in high-rise building using half scale model. A total of thirteen square slab-column specimens, measuring 1100 x 1100 mm with variable thicknesses, constructed and tested in the Advanced Composite Materials Research Laboratory, Benha University, Faculty of Engineering at Shoubra and were designed to fail in punching. All columns were cast monolithically at the center of the slab with 200 mm square section and extended above the slab by 200 mm. The main flexural reinforcement of the slab is uniformly spaced using 7  $\Phi$  12 bars in both directions as a bottom reinforcement mesh, and 6  $\Phi$  10 in both directions as a top reinforcement mesh. Column is reinforced with 4  $\Phi$  12 with two stirrups 8 mm diameter. Figures 1, 2, 3, and 4 show typical specimen details. Table 1 summarizes the studied parameters with one control specimen S1 having slab thickness 120 mm, one row of suggested steel system with length equal to 3  $t_s$ , and S.I.B 100 mm inside the composite column.

#### **3.2 Instrumentation**

The experimental model consists of a typical slab-column system supported on square horizontal steel frame all over the four edges. Loading of all slabs is performed using 1000 kN testing machine through a square steel plate 400 x 400 mm with thickness 40 mm placed over the column stub. Deflection and strains are recorded using LVDT (Linear-Variable-Differentials-Transducer) connected to data acquisition system controlled by computer system. Figure 5 shows the instrument test setup.

#### **3.3 Materials**

A trial mix design has been conducted using locally available materials. The mixes are designed to get target cubic compressive strength greater or equal 40 MPa after 28 days. The materials used for concrete mix are fine aggregate, coarse aggregate, cement, water, and additives (sikament type N). Table 2 shows proportions of concrete mix for the concrete used. Different reinforcement diameters and types (High tensile steel bars with 10 mm and 12 mm diameter and mild steel with 8 mm diameter) with yield strength  $f_y = 420$  MPa and  $f_y = 240$  MPa, respectively, were used for all specimens.

#### **3.4 Experimental Results: Observations and Interpretations**

Table 3 shows the measured first cracking loads, failure loads, and central deflection at failure. Figure 6 shows the typical crack patterns of all specimens. The load deflection curves illustrated in Figure 7, while the maximum concrete strains measured showed in Figure 8.

Based on the test results for the range of the studied factors and from Table 3 and Figures 6, 7, and 8, the following conclusions and observations can be made:

- 1- The failure of all specimens was characterized by a noticeable drop in the sustained load and accompanied by extensive and wide cracks, visible movement of the truncated concrete cone surrounding the steel system.
- 2- The use of the suggested steel system enhanced failure load and wider punching failure surface than that of specimen without steel system.
- 3- For group (1), the increase in slab thickness from 100 mm to 120 mm and 150 mm enhanced the failure load by about 46 %, and 85%, respectively without significant change in the cracking patterns.
- 4- For group (2), although increasing in failure load for specimens S4 and S5 wasn't significant, the cracking patterns of these specimens were closely to regular square shape of punching surface with similar initial cracks compared to control specimen S1.
- 5- For group (3), the increase of the steel section size inside the composite column from S.I.B 80 to S.I.B 100 and S.I.B 120 enhanced the failure load by about 24.5% and 25%, respectively without significant change in the cracking patterns.
- 6- For group (4), where specimens S8 and S9 provided with longer steel system length, exhibited larger perimeters of punching. The radii of the punching surfaces for specimens S8 and S9 were approximately 420 mm and 500 mm, respectively at the bottom face of the slab. The cracking patterns were similar to the corresponding control specimen S1. However, the cracking density was higher and the failure surfaces had obviously wider perimeters than the control specimen did. The enhancement in the failure load was about 4 % and 7 % for specimens S8 and S9, respectively.
- 7- For group (5), there was no significant effect on the cracking pattern due to increasing angle size of the proposed steel system. The enhancement of failure load for specimens S10 and S11 was about 5 % and 18 %, respectively compared to control specimen S1.
- 8- For group (6), long time has been taken to reach failure load of specimen S12 with double rows of steel system compared to specimen S3 which had the same thickness and single row. The failure load enhancement was about 12.5% without significant change of crack pattern.
- 9- For group (7), a significant enhancement in the failure load was recorded particularly for control specimen S1 compared to specimen S13 which had no steel system. The increase in the failure load was about 13.45%. Failure patterns for specimen S13 was different from that of the corresponding control specimen. Yet, the control specimen S1 was obviously has wider cracks.
- 10- The pre-peak load-deflection relationships are shown to be comparable with almost linear response up to the peak load.
- 11- The effect of the slab thickness on the pre and post responses of the slab can be noticed. As expected, increasing the slab thickness is shown to increase significantly the slab punching resistance.
- 12- The change of the steel shape had an insignificant effect on the load-deflection response. The slopes of the curves are tending to be almost identical for specimens in all stages of loading. The maximum deflection is shown to be increased for circular steel section (specimen S4) while to be decreased for box steel section (specimen S5) when compared to control specimen S1.

- 13- Increasing in steel section size (from S.I.B 80 to S.I.B 100 and S.I.B 120) increasing the failure load. However, the deflection responses for specimen S1 had more ductile behavior than others.
- 14- Figure 7(e) shows the effect of the steel system length, where the slope of the curves is similar up-to about 30 % of failure load, then an obviously change for specimens S8 and S9 was recorded. The deflection curve of specimen S8 exhibited higher deflection. Its post-peak behavior was ductile, being characterized by the long plateau developed after the peak load.
- 15- The effect of increasing the steel system angle size (from angle 20x20x2 mm to 30x30x3 mm and 40x40x4 mm) as shown in Figure 7(f) is remarkable, especially on post-peak behavior without significant effect on deflection.
- 16- Comparable conduct was recorded for specimen S12 provided with double rows of steel system (Figure 7(g)). Specimen S12 with double rows exhibited more load resistance behavior up to the peak load compared to specimen S3 with single row, where long plateau developed after the peak load.
- 17- The maximum measured concrete compressive strain value is 0.0025 for specimen S8, while the minimum compressive strain value is 0.0012 for specimen S2.
- 18- The increasing of slab thickness, steel section size, and steel system number of rows had a direct proportional relationship with the concrete compressive strain.
- 19- A significant effect on the concrete compressive strain was clear when increasing the steel system length and steel angles size compared to the control specimen S1. However, continuous increasing of strains gives an opposite result as shown for specimens S9 and S11.

## **4- NUMERICAL STUDY**

### **4.1 Finite Element Idealization Using “ANSYS 8” Program**

#### **4.1.1 Solid 65 3-D Element**

Solid 65 is used for the three-dimensional modeling of solids with or without reinforcing rebars. The element is capable of cracking in tension and crushing in compression. The solid element capability may be used to model reinforced and unreinforced concrete, while the rebar capability is available for modelling reinforcement behaviour.

#### **4.1.2 Shell 63 Element**

Shell 63 has both bending and membrane capabilities may be used to model steel sections. Both in-plane and normal loads are permitted. The element has six degrees of freedom at each node: translations in the nodal x, y, and z directions and rotations about the nodal x, y, and z-axes.

### **4.2 Analysis of Results**

Numerical results using “ANSYS 8” program are found to be conforming to those given experimentally, (Figures 9 and 10), where the comparison shows good agreement

between the experimental and the numerical results for the failure loads, within a difference between 1 % to 10 % as shown in Table 4, which is acceptable.

## **5- PARAMETRIC STUDY**

### **5.1 General**

“ANSYS 8” program is used for parametric studies to further extent the understanding of the mechanism of composite column-flat slab connection under static vertical loading and provide information that cannot be easily measured in experimental studies.

The specimens used throughout the present work selected such that their dimensions, boundary conditions, loading and material properties chosen to represent common practice in buildings used in Egypt within the practical limits. Figure 11 shows concrete dimensions and reinforcement details for the control numerical model.

### **5.2 Studied Factors**

The influence of the different key factors affecting the nonlinear behavior and performance of composite column-flat slab connection under vertical loading has been investigated. The main key factors investigated throughout this study are: (1) concrete compressive strength “ $f_{cu}$ ”; (2) steel reinforcement yield strength “ $f_y$ ”; (3) column rectangularity ratio; (4) concrete slab rectangularity ratio; (5) reinforcement steel ratio “ $\mu$ ”; (6) different steel system lengths with double number of rows, in addition to practice dimensions for: (7) slab thickness; (8) steel system size; (9) shape of the steel section inside the composite column; (10) size of the steel section inside the composite column; (11) steel system lengths inside the concrete flat slab; and (12) steel system number of rows. The values of the studied factors shown in Table 5.

### **5.3 Analysis of the Numerical Results**

#### **5.3.1 General**

To address the research objectives, the calculated loads and deflections at failure compared with those of the corresponding control model. Table 5 illustrates the effect of the studied parameters on the behavior.

#### **5.3.2 Effect of compressive strength ( $f_{cu}$ )**

From Table 5, it can be concluded that increasing of concrete compressive strength “ $f_{cu}$ ” from 25 to 27.5, 30, and 35 MPa, increasing the failure load by about 20 %, 38 %, and 56 %, respectively.

#### **5.3.3 Effect of reinforcement steel yield strength ( $f_y$ )**

Increasing yield strength of reinforcing steel from 360 to 420 MPa were slightly affecting the failure load capacity. It can be neglected specially at early stages of loading history. At load about 75% of failure load, the model with reinforcing steel

yield strength of 420 MPa shows an increasing in loading until reached failure by about 5%. Changing of central deflection can be neglected.

### **5.3.4 Effect of bottom reinforcement steel ratio ( $\mu$ )**

The failure load for ( $\mu = 0.75 \mu_{\max}$ ) and ( $\mu = \mu_{\max}$ ) is enhanced by about 28% and 43%, respectively compared to the control model where ( $\mu = 0.5 \mu_{\max}$ ). However, the central deflection decreased by increasing the bottom reinforcement steel ratio. The reduction was about 5% and 17% for ( $\mu = 0.5 \mu_{\max}$ ) and ( $\mu = 0.75 \mu_{\max}$ ), respectively.

### **5.3.5 Effect of steel system angles lengths**

Generally, increasing the steel system length, enhance punching failure load. The failure load enhanced by about 6 %, 13 %, and 19 % while the central deflection increased by about 5 %, 9 %, and 16 % when increasing steel system length from 280 to 600, 800, and 1000 mm, respectively.

### **5.3.6 Effect of steel system angles size**

No significant effect can be found when increasing steel system angles size at the first loading stages. However, slight increase was found for the failure load by about 3 %, 5 %, and 6 %, also central deflection increased by about 2 %, 4 %, and 7 % was observed when increasing angles size from 30x30x3 mm to 40x40x4, 50x50x5, and 60x60x6 mm, respectively.

### **5.3.7 Effect of steel section size**

No significant effect was recorded at different load stages when changing steel section size. Slightly enhancement about 1 % on the failure load was recorded when increasing steel section from S.I.B 200 to S.I.B 260, also from S.I.B 260 to S.I.B 300.

### **5.3.8 Effect of column dimensions**

Increasing rectangularity ratio of column dimensions from 1.0 to 1.25, 1.5, and 2.0, increasing the failure load by about 4%, 7%, and 12%, respectively, while the central deflection decreased by about 1.2%, 3%, and 6%, respectively.

### **5.3.9 Effect of slab thickness**

As expected, changing slab thickness has a significant enhancement effect on the punching resistance. It can be noticed that, changing the slab thickness from 180 to 200, 220, and 250 mm increases the failure load by about 18 %, 32 %, and 58 %, respectively.

### **5.3.10 Effect of slab dimensions**

Insignificant effect was recorded at the early stages of loading until reaching about 30 % of failure load of control model. Higher response was observed for rectangularity ratio

equals to 1.0. Increasing rectangularity ratio to 1.25, decreasing failure load by about 7 %. When changing rectangularity ratio from 1.0 to 1.5 and 2.0 the slopes of the load deflection curves tend to be almost identical in the stages of loading without significant difference of failure load.

### 5.3.11 Effect of steel system (number of rows)

Using two rows of steel system, increasing the failure load by about 3 % compared to the control model where one row of steel system used. While using two rows and increasing the length of the bottom row to be 1200 mm, increasing the failure load by about 15 % compared to the control model. Small reduction in central deflection (which can be neglected) was recorded when using two rows of steel system with different lengths.

## 6- PROPOSED EQUATION

The Euro code equation is simple and capable of predicting concrete contribution covering the effective parameters as slab thickness, concrete compressive strength, and flexure steel reinforcement ratio. The contribution of concrete stress and the maximum punching shear resistance of flat slab are given form equations 1 and 2:

$$V_c = v_c u d \quad (1)$$

$$v_c = 0.12 k (100\rho f_c)^{1/3} \geq 0.035 k^{3/2} f_c^{1/2} \quad (2)$$

Where:

$$k = (1 + (200/d))^{1/2} \geq 2$$

$d$  is the depth of the concrete flat slab;

$\rho$  is the mean flexural reinforcement ratio not more than 2.0%;

$f_c$  is the concrete compressive strength;

$u$  is the critical perimeter at  $2d$  from the column.

Starting from the previous equations, and based on the numerical results obtained from the parametric study, an equation to calculate the contribution of steel system is introduced. This equation evaluate the punching shear resistance by the steel system as a function of steel system angle length ( $L_s$ ) which is the most effective parameter, and the angles size of the steel system ranged between 0.15 to 0.3 slab thickness. The developed equation is:

$$V_{ss} = (4.7897) \cdot (L_s)^{0.498} \quad (3)$$

Where:

$V_{ss}$  is the punching shear resistance by the steel system;

$L_s$  is the length in (mm) for one steel angle.



From equations (1) and (3), the punching shear resistance for the composite column-flat slab connection provided by the suggested steel system in this study ( $V_{cs}$ ) can evaluate from following equation:

$$V_{cs} = V_c + V_{ss} \quad (5)$$

The verification and comparison of the previous equation with the experimental, numerical, and parametric study results is shown in Figure 12.

## 7- CONCLUSION

- 1- The cracks pattern was comparable for all the specimens provided with the suggested steel system. Specimens provided with longer steel system exhibited larger perimeters of punching compared to the control specimen without a significant change in the cracking pattern.
- 2- Enhancement in the failure load was recorded for specimens provided with the suggested steel system. The enhancement ranging between 2.53% and 33.5%.
- 3- Changing the steel section shape from S.I.B to box and circular tube inside the composite column had no significant effect on the failure load. While increasing steel section size inside the composite column from S.I.B-80 to S.I.B-100 and S.I.B-120 enhanced the failure load by 24.5% and 25%, respectively.
- 4- Increasing the length of the reinforcing angles from 3 times the slab thickness to 4 and 5 times the thickness enhanced the failure load by about 4% and 7%, respectively, while increasing the angles size from 20x20x2 mm to 30x30x3 mm and 40x40x4 mm increased the failure load by about 5% and 18%, respectively.
- 5- Doubling the reinforcing angles rows enhanced the failure load by about 12.5% when compared to the specimen with one row of angles.
- 6- Increasing the slab thickness from 100 mm to 120 mm and 150 mm enhanced the failure load by 46%, and 85%, respectively.
- 7- All the specimens failed in a punching shear mode with a brittle manner and a sudden loss of capacity. The use of steel system resulted in a wider punching failure surface than that of the specimen without the suggested reinforcing system.
- 8- The maximum recorded concrete strain for the test specimens was 0.0025, and none of strain gages reached the crushing strain values stated in the codes.
- 9- For the range of the investigated test parameters, the application of non-linear finite elements method using “ANSYS V.8” package, yielded superior results including the cracking pattern, load-carrying capacity, and load-deflection response.
- 10- The analytical load-carrying capacity of the composite column-flat slab connection was considerably affected by the concrete compressive strength. An increase of about 20%, 38%, and 56% in the failure load was obtained by increasing the compressive strength from 25 MPa to 27.5 MPa, 30 MPa, and 35 MPa, respectively.
- 11- Increasing the yield strength of the tension reinforcement steel from 360 MPa to 420 MPa was slightly affected the failure load capacity. The predicted failure load was enhanced by about 5%.
- 12- Increasing the tension reinforcement steel ratio had a significant effect on the punching resistance. The analytical failure load of the slabs provided with 0.75

$\mu_{max}$  and  $\mu_{max}$  was 1.28 and 1.43, respectively, times that of the control slab which provided with 0.5  $\mu_{max}$ .

- 13- Enhancement of the predicted failure load was about 3.5%, 13%, and 12% when increasing column dimensions from 400x400 mm to 400x500 mm, 400x600 mm, and 400x800 mm, respectively.
- 14- Increasing the slab rectangularity ratio from 1.0 to 1.25 resulted in a 7% reduction in the predicted failure load. The slopes of the load-deflection curves were observed to be almost identical throughout the loading stages without significant difference in the failure load when changing rectangularity ratio from 1.0 to 1.5 and 2.0.
- 15- Using two rows of the reinforcing angles increased the failure load by about 3% compared to the control slab where one row of angles was provided.

## REFERENCES

- [1] Piel W., Hanswille G. (2006), "**Composite Shear Head Systems for Improved Punching Shear Resistance of Flat Slabs**", ASCE books publications, Composite Construction in Steel and Concrete V, pp. 226-235.
- [2] Swamy R. N. and Ali S. A. R. (1982), "**Punching Shear Behavior of Reinforced Slab-Column Connections Made with Steel Fiber Concrete**", ACI Structural Journal, V. 79, No. 5, September-October 1982, pp. 392-406.
- [3] El-Salakawy E. F., Polak M. A., and Soudki K. A. (2003), "**New Shear Strengthening Technique for Concrete Slab-Column Connections**", ACI Structural Journal, V. 100, No. 3, May-June 2003, pp. 297-304.
- [4] Oliveira D. R., Melo G. S., and Regan P. E. (2000), "**Punching Strengths of Flat Plates with Vertical or Inclined Stirrups**", ACI Structural Journal, V. 97, No. 3, May-June 2000, pp. 485-491.
- [5] Osman M., Marzouk H., and Helmy S. (2000), "**Behavior of High-Strength Lightweight Concrete Slabs under Punching Loads**", ACI Structural Journal, V. 97, No. 3, May-June 2000, pp. 492-498.
- [6] Hegger J., Sherif A. G., and Ricker M. (2006), "**Experimental Investigations on Punching Behavior of Reinforced Concrete Footings**", ACI Structural Journal, V. 103, No. 4, July-August 2006, pp. 604-613.
- [7] Muttoni A. (2008), "**Punching Shear Strength of Reinforced Concrete Slabs without Transverse Reinforcement**", ACI Structural Journal, V. 105, No. 4, July-August 2008, pp. 440-450.
- [8] Ospina C. E., Alexander S. D. B., and Cheng J. J. R. (2003), "**Punching of Two-Way Concrete Slabs with Fiber-Reinforced Polymer Reinforcing Bars or Grids**", ACI Structural Journal, V. 100, No. 5, September-October 2003, pp. 589-598.

- [9] Ghali A. and Megally S. (1999), "**Design for Punching Shear Strength with ACI 318-95**", ACI Structural Journal, V. 96, No. 4, July-August 1999, pp. 539-549.
- [10] Vainiūnas P., Popovas V. and Jarmolajev A. (2002), "**Punching Shear Behavior Analysis of RC Flat Floor Slab-To-Column Connection**", Journal of Civil Engineering and Management, Vol. VIII, No. 2, pp. 77-82.
- [11] Sarnoa L. Di, Peccea M.R., Fabbrocinob G. (2007), "**Inelastic Response of Composite Steel and Concrete Base Column Connections**", Journal of Constructional Steel Research, V. 63, pp. 819-832.
- [12] Roberts E. H. and Yam L. C. B. (1983), "**Some Recent Methods for the Design of Steel, Reinforced Concrete, and Composite Steel-Concrete Columns in the U.K.**", ACI Structural Journal, V. 80, March-April 1983, pp. 139-149.
- [13] Mensch L. J. (1930), "**Composite Columns**", ACI Structural Journal, March-April 1930, pp. 263-280.
- [14] Mu B. and Meyer C. (2003), "**Bending and Punching Shear Strength of Fiber-Reinforced Glass Concrete Slabs**", ACI Structural Journal, V. 100, No. 2, March-April 2003, pp. 127-132.
- [15] Naaman A. E., Likhitrungsilp V., and Montesinos G. P. (2007), "**Punching Shear Response of High-Performance Fiber-Reinforced Cementitious Composite Slabs**", ACI Structural Journal, V. 104, No. 2, March-April 2007, pp. 170-179.
- [16] Bazant Z. P. and Cao Z. (1985), "**Size Effect in Punching Shear Failure of Slabs**" ACI Structural Journal, V. 84, January-February 1985, pp. 44-53.
- [17] Alexander S. D. B. and Simmonds S. H. (1992), "**Tests of Column-Flat Plate Connections**", ACI Structural Journal, V. 89, No. 5, September-October 1992, pp. 495-502.
- [18] Menétrey P. (1996), "**Analytical Computation of the Punching Strength of Reinforced Concrete**", ACI Structural Journal, V. 93, No. 5, September-October 1996, pp. 1-9.
- [19] Bortolotti L. (1990), "**Punching Shear Strength in Concrete Slabs**", ACI Structural Journal, V. 87, No. 2, March-April 1990, pp. 208-219.
- [20] Shukry M. E. S. and Goode C. D. (1990), "**Punching Shear Strength of Composite Construction**", ACI Structural Journal, V. 87, No. 1, January-February 1990, pp. 12-22.

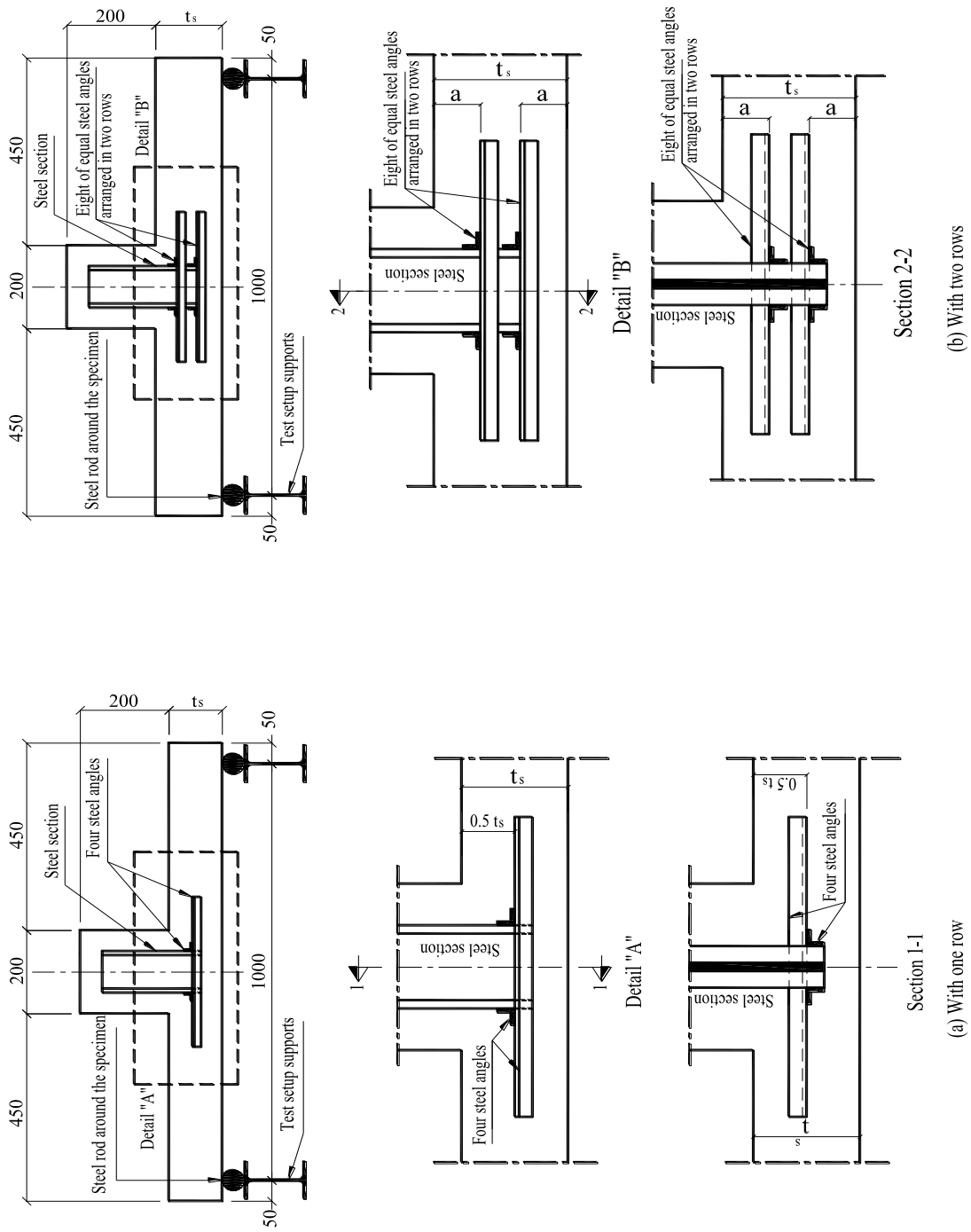
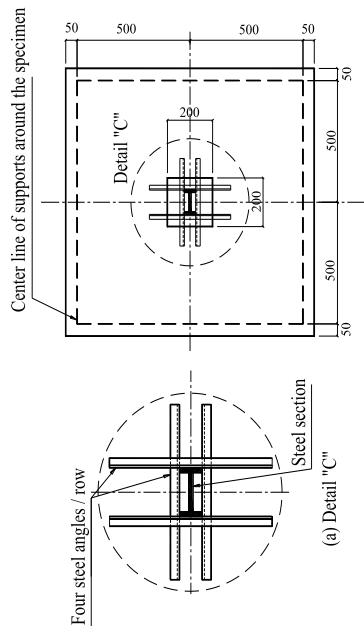


Figure 1 Typical section for the specimen for one and two rows



(a) Typical plan view for the specimen



(b) Photographs for some specimens

Figure 2. Test specimens

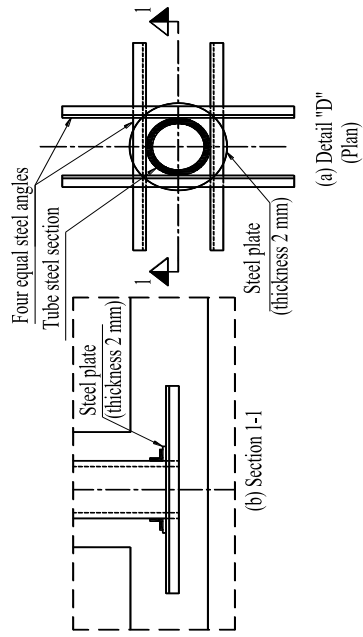


Figure 3 Steel system detail for circular (tube) steel section

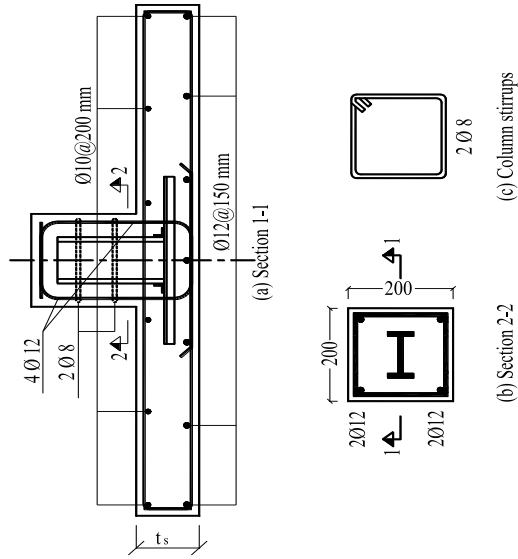


Figure 4 Typical specimen reinforcement details

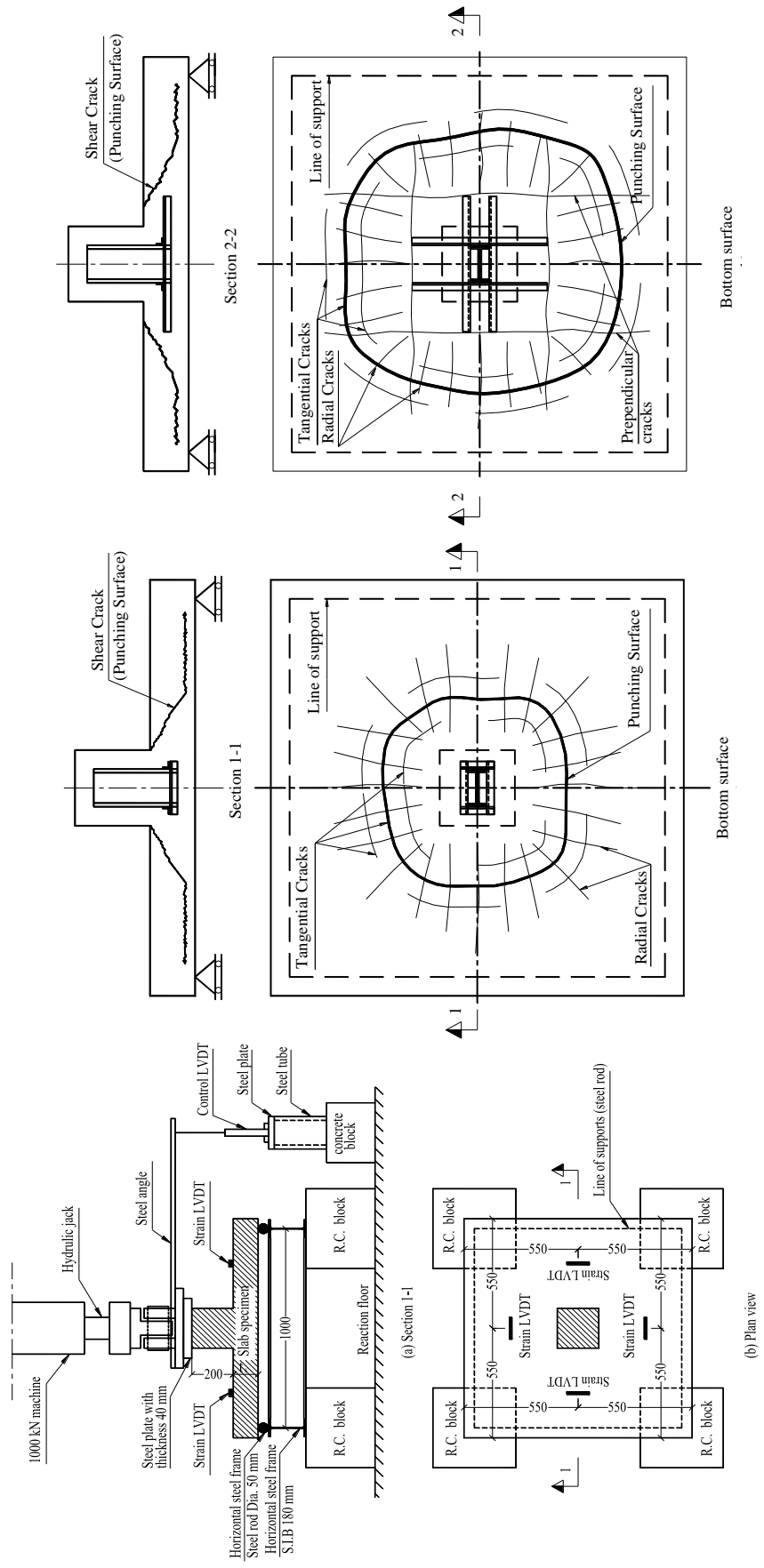
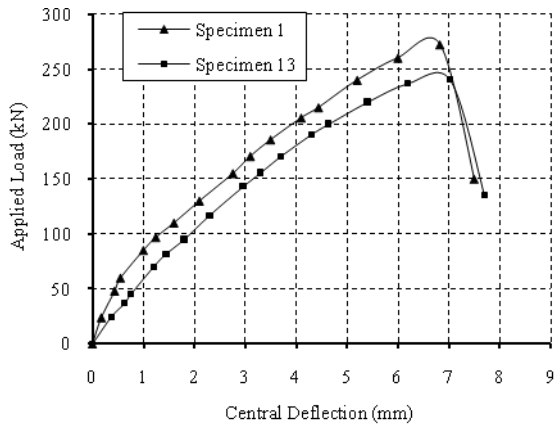


Figure 5 Instrumentation and test setup

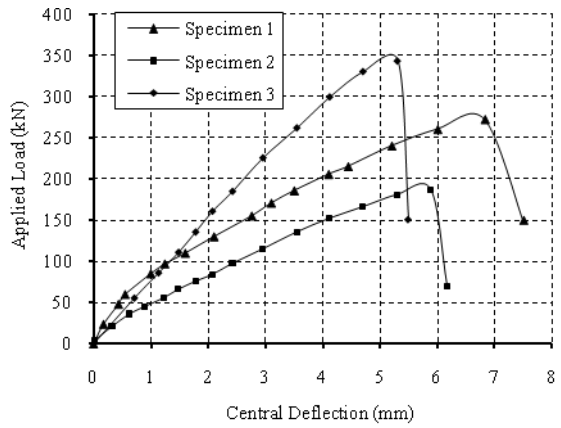
(a) Crack pattern without suggested steel system

(b) Crack pattern with suggested steel system

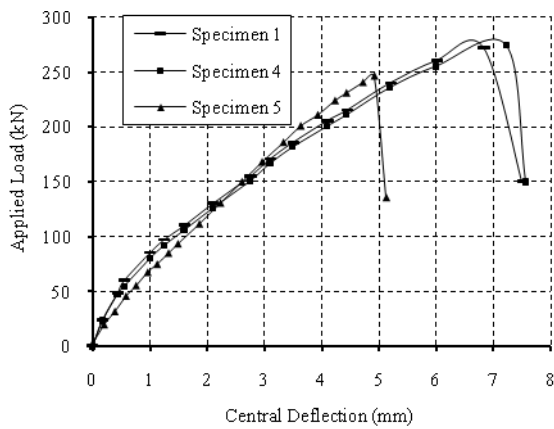
Figure 6 Crack pattern for specimen with and without steel system



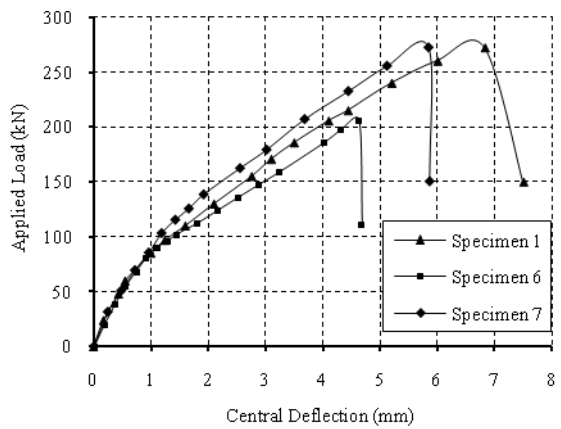
(a) Effect of steel system



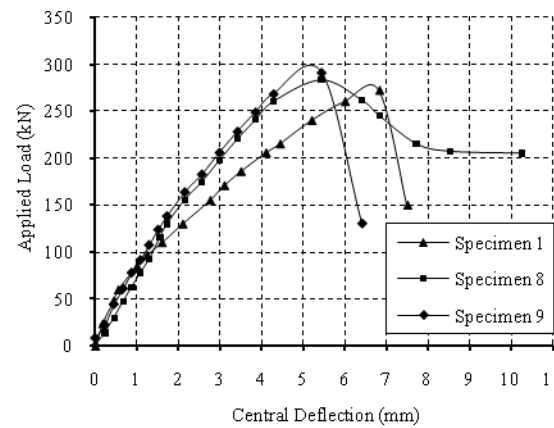
(b) Effect of slab thickness



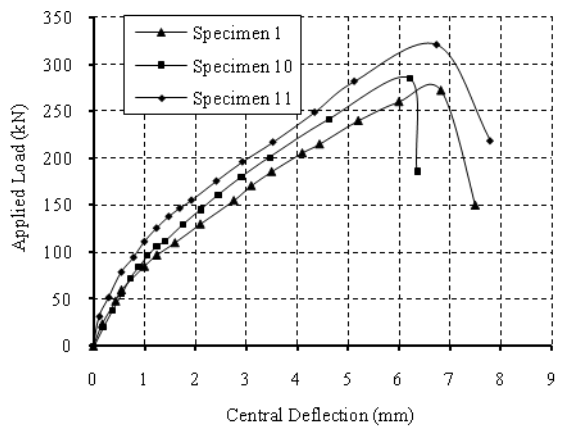
(c) Effect of steel section shape inside the composite column



(d) Effect of steel section size inside the composite column

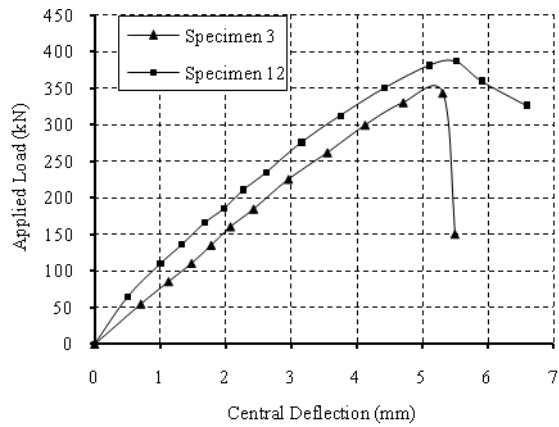


(e) Effect of steel system angles lengths



(f) Effect of steel system angles size

Figure 7 Load deflection curves for the experimental parameters effects



(g) Effect of steel system number of rows  
Figure 7 (Continues)

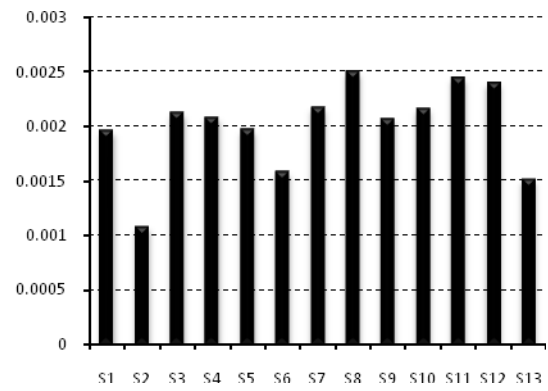
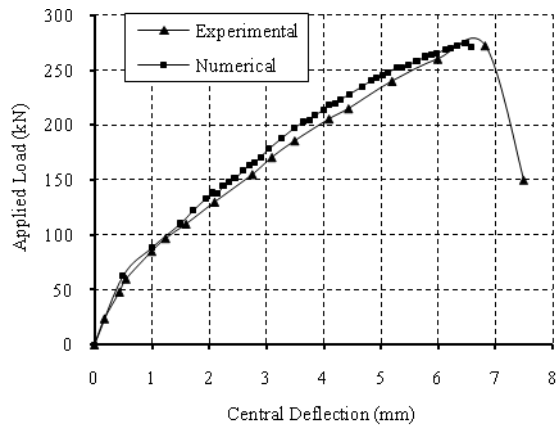
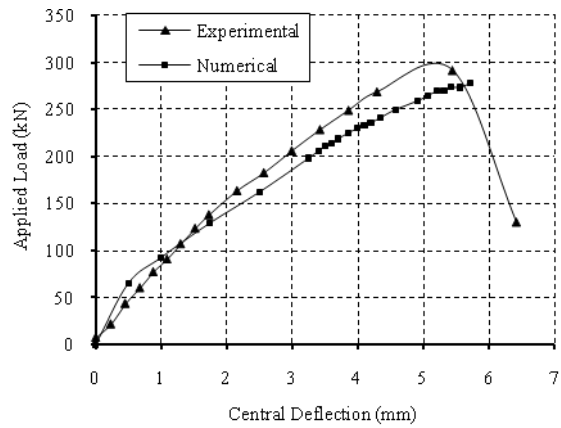


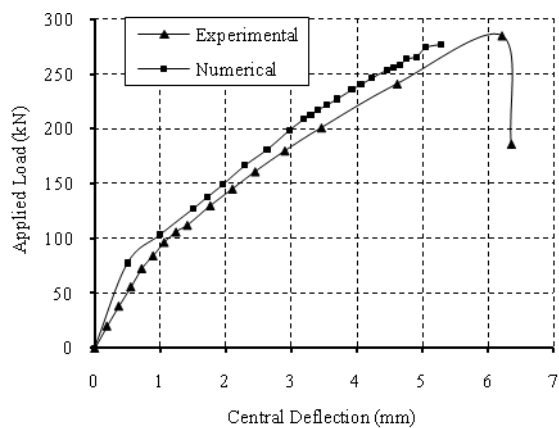
Figure 8 Maximum concrete compressive strains for specimens



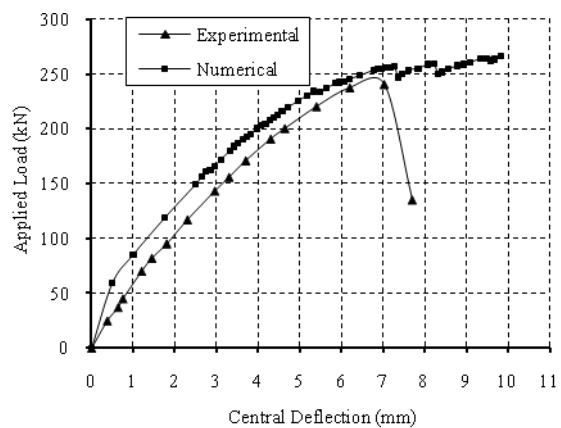
Specimen 1



Specimen 9



Specimen 10



Specimen 13

Figure 9 Load deflection curves for the experimental and numerical results for some specimens



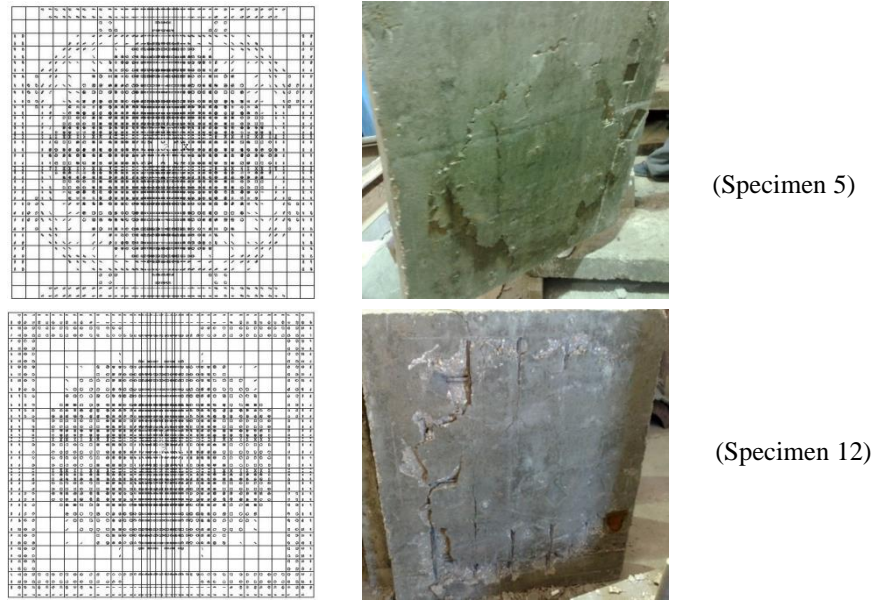


Figure 10 Comparison between experimental and numerical failure mode for specimens S5 and S12

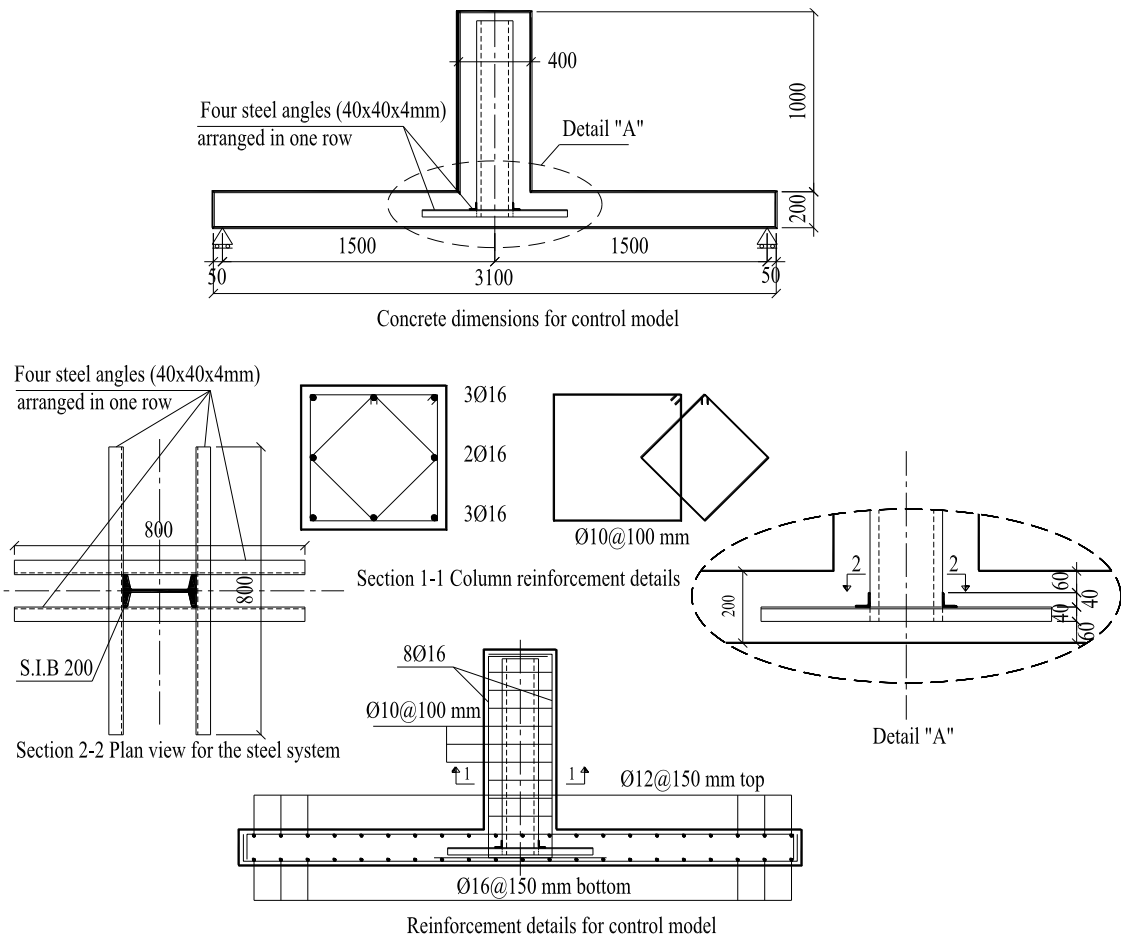


Figure 11 Concrete dimensions and reinforcement details for control model

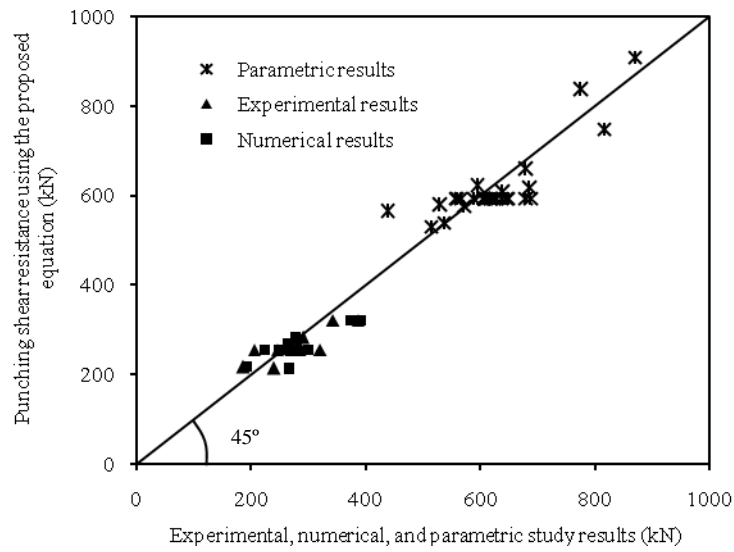


Figure 12 Verification of the proposed equation with the experimental, numerical, and parametric study results

Table 1 Experimental studied parameters

Specimen Model	Group number	Evaluated criteria	Slab thickness (mm)	Suggested steel system				Steel section inside composite column	
				No. of angles	Angle length (mm)	Angle size (mm)	No. of rows	Type	Size (mm)
S1	Control specimen	Control specimen	120	4	360	20x20x2	1	S.I.B	100
S2	1	Slab thickness	100	4	360	20x20x2	1	S.I.B	100
S3			150	4	360	20x20x2	1	S.I.B	100
S4	2	Shape of steel section inside composite column	120	4	360	20x20x2	1	Tube	Dia. 100
S5			120	4	360	20x20x2	1	Box	100 x 100
S6	3	Size of steel section inside composite column	120	4	360	20x20x2	1	S.I.B	80
S7			120	4	360	20x20x2	1	S.I.B	120
S8	4	Length of the steel system	120	4	480	20x20x2	1	S.I.B	100
S9			120	4	600	20x20x2	1	S.I.B	100
S10	5	Size of the steel system	120	4	360	30x30x3	1	S.I.B	100
S11			120	4	360	40x40x4	1	S.I.B	100
S12	6	No. of steel system rows	150	8	360	20x20x2	2	S.I.B	100
S13	7	Without steel system	120	4	100	20x20x2	1	S.I.B	100

Table 2 Concrete components

Fine agg. Sand (Kg)	Coarse agg. Size 1 (Kg)	Cement (Kg)	Water (Kg)	Additive Sikament type N (Kg)
780	980	340	160	5

Table 3 Tests results

Specimen number	Group number	Evaluated criteria	First crack load (kN)	Failure load (kN)	Deflection at failure (mm)
S1	Control specimen	Control specimen	54.47	272.33	6.83
S2	1	Effect of slab thickness	24.27	186.70	5.31
S3			103.15	343.82	5.31
S4	2	Effect of steel section shape	63.10	274.33	7.23
S5			49.28	246.41	4.91
S6	3	Effect of steel section dimension	38.47	205.70	4.63
S7			57.20	272.38	5.84
S8	4	Effect of suggested steel system length	79.28	283.16	5.44
S9			87.35	291.16	5.44
S10	5	Effect of suggested steel system sections	57.01	285.06	6.21
S11			64.18	320.92	6.74
S12	6	Effect of no. of steel system rows	123.78	386.82	5.51
S13	7	Without steel system	48.07	240.33	7.03

Table 4 Comparison between test results and numerical results

Specimen No.	Failure load			Deflection at failure		
	Experimental $P_{exp}$ (kN)	Numerical $P_n$ (kN)	$P_n / P_{exp}$	Experimental $\Delta_{exp}$ (mm)	Numerical $\Delta_n$ (mm)	$\Delta_n / \Delta_{exp}$
1	272.33	274.59	1.01	6.83	6.48	0.95
2	186.70	193.15	1.03	5.31	5.45	1.03
3	343.82	374.84	1.09	5.31	5.53	1.04
4	274.33	278.59	1.02	7.23	6.48	0.90
5	246.41	249.90	1.01	4.91	5.14	1.05
6	205.70	224.27	1.09	4.63	4.76	1.03
7	272.38	263.30	0.97	5.84	5.04	0.86
8	283.16	265.41	0.94	5.44	5.33	0.98
9	291.16	277.32	0.95	5.44	5.72	1.05
10	285.06	267.01	0.94	6.21	5.27	0.85
11	320.92	300.85	0.94	6.74	6.84	1.02
12	386.82	391.05	1.01	5.51	5.18	0.94
13	240.33	266.40	1.11	7.03	9.84	1.40

Table 5 Numerical results for the parametric study

Model No.	Evaluated criteria		Numerical results at failure		Comments
	Variable	Value	Failure load (kN)	Central deflection (mm)	
1	$f_{cu}$ (MPa)	25	438.64	15.34	
2		27.5	529.49	17.33	
3		30	606.09	19.41	Control model
4		35	685.68	17.89	
5	$f_y$ (MPa)	360	606.09	19.41	Control model
6		420	637.81	19.42	
7	Steel system angle lengths (mm)	280	537.29	17.85	
8		600	571.53	18.83	
9		800	606.09	19.41	Control model
10		1000	638.61	20.78	
11	Steel system angle size (mm)	30x30x3	588.63	18.90	
12		40x40x4	606.09	19.41	Control model
13		50x50x5	618.66	20.02	
14		60x60x6	623.35	20.57	
15	Column dimensions (mm)	400x400	606.09	19.41	Control model
16		400x500	627.67	19.14	
17		400x600	648.36	18.81	
18		400x800	678.56	18.23	
19	Slab dimensions (mm)	3000x3000	606.09	19.41	Control model
20		3000x3750	566.23	19.01	
21		3000x4500	559.42	19.86	
22		3000x6000	557.23	18.87	
23	Slab thickness (mm)	180	515.17	21.35	
24		200	606.09	19.41	Control model
25		220	678.82	17.47	
26		250	815.84	16.46	
27	Steel section size S.I.B (mm)	200	606.09	19.41	Control model
28		260	611.00	19.90	
29		300	616.84	21.06	
30	No. of rows	one row	606.09	19.41	Control model
31		two rows	645.13	19.01	
32		two rows with different lengths	688.26	18.72	
33	Steel reinforcement ratio ( $\mu$ )	$\mu = 0.5 \mu_{max}$	606.09	19.41	Control model
34		$\mu = 0.75 \mu_{max}$	774.89	18.38	
35		$\mu = \mu_{max}$	869.65	16.49	